Journal of Solid State Chemistry 182 (2009) 389–395

Contents lists available at ScienceDirect

Journal of Solid State Chemistry

journal homepage: www.elsevier.com/locate/jssc

High-pressure transitions in $MgAl_2O_4$ and a new high-pressure phase of $Mg_2Al_2O_5$

A. Enomoto [a], H. Kojitani [a], M. Akaogi [a,*], H. Miura [b], H. Yusa [c]

[a] Department of Chemistry, Gakushuin University, 1-5-1 Mejiro, Toshima-ku, Tokyo 171-8588, Japan
[b] Division of Earth and Planetary Sciences, Graduate School of Science, Hokkaido University, N10, W8, Kita-ku, Sapporo 060-0810, Japan
[c] Advanced Materials Laboratory, National Institute of Materials Science, 1-1 Namiki, Tsukuba, Ibaraki 305-0044, Japan

ARTICLE INFO

Article history:
Received 22 July 2008
Received in revised form
30 October 2008
Accepted 2 November 2008
Available online 21 November 2008

Keywords:
High pressure
Phase transition
$MgAl_2O_4$
Spinel
$Mg_2Al_2O_5$ phase
Ludwigite

ABSTRACT

Phase transitions in $MgAl_2O_4$ were examined at 21–27 GPa and 1400–2500 °C using a multianvil apparatus. A mixture of MgO and Al_2O_3 corundum that are high-pressure dissociation products of $MgAl_2O_4$ spinel combines into calcium–ferrite type $MgAl_2O_4$ at 26–27 GPa and 1400–2000 °C. At temperature above 2000 °C at pressure below 25.5 GPa, a mixture of Al_2O_3 corundum and a new phase with $Mg_2Al_2O_5$ composition is stable. The transition boundary between the two fields has a strongly negative pressure–temperature slope. Structure analysis and Rietveld refinement on the basis of the powder X-ray diffraction profile of the $Mg_2Al_2O_5$ phase indicated that the phase represented a new structure type with orthorhombic symmetry (*Pbam*), and the lattice parameters were determined as $a = 9.3710(6)$ Å, $b = 12.1952(6)$ Å, $c = 2.7916(2)$ Å, $V = 319.03(3)$ Å^3, $Z = 4$. The structure consists of edge-sharing and corner-sharing (Mg, Al)O_6 octahedra, and contains chains of edge-sharing octahedra running along the *c*-axis. A part of Mg atoms are accommodated in six-coordinated trigonal prism sites in tunnels surrounded by the chains of edge-sharing (Mg, Al)O_6 octahedra. The structure is related with that of ludwigite (Mg, Fe^{2+})$_2$(Fe^{3+}, Al)(BO_3)O_2. The molar volume of the $Mg_2Al_2O_5$ phase is smaller by 0.18% than sum of molar volumes of 2MgO and Al_2O_3 corundum. High-pressure dissociation to the mixture of corundum-type phase and the phase with ludwigite-related structure has been found only in $MgAl_2O_4$ among various $A^{2+}B_2^{3+}O_4$ compounds.

1. Introduction

High pressure transitions in $MgAl_2O_4$ have been a subject of many experimental studies from the viewpoints of both earth science and materials science. Because $MgAl_2O_4$ spinel is one of important rock-forming minerals, its high-pressure behaviors are of considerable interest to clarify host phase of aluminum in the earth's deep mantle [1,2]. In addition, high-pressure transitions of AB_2O_4 compounds with spinel structure are an interesting subject in materials science, because denser phases than AB_2O_4 spinel may have interesting structural features and physical properties as potential functional materials [3,4].

Phase transitions of $MgAl_2O_4$ at high pressures and high temperatures have been studied using multianvil apparatus and diamond anvil cell. At 1200–1600 °C, $MgAl_2O_4$ spinel dissociates at 15–16 GPa to a mixture of MgO periclase and Al_2O_3 corundum, which reacts to form $MgAl_2O_4$ phase with calcium ferrite structure at 25–27 GPa [1]. The calcium ferrite phase further transforms to $CaTi_2O_4$-type structure at about 40 GPa and 2000–3000 °C [2]. However, it was reported that a very dense phase, ε-$MgAl_2O_4$, was synthesized at pressure above about 25 GPa at about 1000 °C [5] and that ε-$MgAl_2O_4$ transformed to $CaTi_2O_4$ phase at 45–50 GPa at 1100–2500 °C [6]. These results suggest that experimental data above about 25 GPa are still controversial. Also, high-pressure experimental study on $MgAl_2O_4$ at pressures of 20–30 GPa and temperature above 2000 °C has not yet been reported.

In this study, we have examined the phase relations in $MgAl_2O_4$ in the pressure range of 21–27 GPa at temperatures of 1400–2500 °C using a multianvil apparatus. We have found a new high-pressure phase with $Mg_2Al_2O_5$ composition and have analyzed its crystal structure. The results of the phase relations in $MgAl_2O_4$ are shown, and the structure of the new $Mg_2Al_2O_5$ phase is discussed.

2. Experimental methods

$MgAl_2O_4$ spinel was synthesized from an intimate mixture of reagent grade MgO and Al_2O_3 with 1:1 molar ratio by heating at

* Corresponding author. Fax: +81 3 5992 1029.
E-mail address: masaki.akaogi@gakushuin.ac.jp (M. Akaogi).

0022-4596/$ - see front matter © 2008 Elsevier Inc. All rights reserved.
doi:10.1016/j.jssc.2008.11.015

1400 °C for 100 h. By examining with a powder X-ray diffractometer and a scanning electron microscope with an energy-dispersive spectrometer (SEM-EDS), the product was confirmed to be single-phase $MgAl_2O_4$ with spinel structure. The $MgAl_2O_4$ spinel was used as the starting material for most of high-pressure experiments. An intimate mixture of MgO and Al_2O_3 with 2:1 molar ratio was also used as the starting material for the runs of $Mg_2Al_2O_5$ composition.

High-pressure experiments were carried out using a Kawai-type multianvil apparatus at Gakushuin University. Tungsten carbide anvils with truncated edge lengths of 1.5 and 2.5 mm were used together with MgO octahedra of 4.7 and 7 mm in edge, respectively, as pressure media. A cylindrical Re furnace was put in the central part of the octahedron. A $LaCrO_3$ sleeve was inserted between the heater and the pressure medium for thermal insulation. The powdered starting material was put into the central part of the furnace together with $LaCrO_3$ plugs at both ends. Two Re discs were inserted between the starting material and the $LaCrO_3$ end-plugs to avoid reaction between them. Temperature was measured at the central part of the furnace with a Pt/Pt-13%Rh thermocouple or a W-3%Re/W-25%Re thermocouple. When the Pt/Pt-13%Rh thermocouple was used, temperature below 1800 °C was measured directly by the electromotive force (emf) of the thermocouple, and temperature above 1800 °C was estimated by extrapolating the power-temperature relationship obtained at 1000–1800 °C at heating stage of each run. In the runs using the W-3%Re/W-25%Re thermocouple, temperature was directly measured from the emf. No correction was made on pressure effect of the emf. Although temperature above 1800 °C was estimated in the runs of the Pt/Pt-13%Rh thermocouple, it was shown that transition boundary between periclase+corundum and $Mg_2Al_2O_5$ phase+corundum determined by the Pt/Pt-13%Rh thermocouple at 23 GPa at 2000–2100 °C was consistent with that by the W-3%Re/W-25%Re thermocouple. Therefore, uncertainty of temperature above 1800 °C was estimated to be within about $\pm$50 °C, when temperature was estimated from the power-temperature relationship. Below 1800 °C, the temperature uncertainty was estimated to be within about $\pm$20 °C. Pressure was calibrated at room temperature using pressure-fixed points of ZnS (15.5 GPa), GaAs (18.3 GPa) and GaP (23 GPa). The pressure at high temperature was corrected using phase transition boundaries of α–β and β–γ transitions in Mg_2SiO_4 [7,8], ilmenite–perovskite transition in $MgSiO_3$ [9], and dissociation of $Mg_3Al_2Si_3O_{12}$ pyrope to perovskite plus corundum [10]. Relative uncertainty in pressure was estimated to be about $\pm$0.3 GPa.

The sample was kept at pressure–temperature conditions with a certain period, quenched under pressure, and recovered to ambient conditions. The recovered sample was fixed on a slide glass with an epoxy resin, and polished into flat. Phase identification was performed in the area near the thermocouple junction within about 0.1 mm in the central part of each sample, using a microfocus X-ray diffractometer with an X-ray beam collimated to 50 μm in diameter. Some recovered samples were crushed into powder, and examined by the powder X-ray diffractometer. In both of the microfocus and powder X-ray diffraction experiments, X-ray diffraction profiles were measured by the X-ray diffractometer (Rigaku RINT2500 V) operated at 45 kV and 250 mA with monochromatized Cr$K\alpha$ X-ray. Compositions of phases in some run products were analyzed by the scanning electron microscope (JEOL JMS-6360) with the energy-dispersive spectrometer (Oxford INCA *x*-sight). The scanning electron microscope was operated with acceleration voltage of 15 kV and probe current of 0.35 nA. The electron beam diameter was about 1 μm. The analysis data of 8–22 points were averaged with two standard deviations of the mean. Synthetic $Mg_3Al_2Si_3O_{12}$ pyrope [11] was used as the standards of Mg, Al and Si.

The $Mg_2Al_2O_5$ high-pressure phase was synthesized by keeping the mixture of MgO and Al_2O_3 with 2:1 mol ratio at 23–24 GPa and 2500 °C for 1–10 min. One of the run products (run no. N-6) was carefully examined by microfocus X-ray diffraction to confirm as the single-phase material. Then, it was crushed using a WC die at liquid nitrogen temperature, and ground in an agate mortar. The powdered sample was mounted on a non-reflective quartz plate. To collect the X-ray profile for structural analysis of the $Mg_2Al_2O_5$ phase, the X-ray diffractometer was operated by the step-scan method in the 2θ range of 20–140°. The step size and counting time were 0.02° and 15 s, respectively. Si powder was used as the 2θ standard. The obtained X-ray diffraction profile was analyzed by the Rietveld method using a program RIETAN-2000 [12]. A structure model for the Rietveld analysis was based on structure of ludwigite (Mg, Fe^{2+})$_2$(Fe^{3+}, Al)(BO_3)O_2 [13] with considerable modification, as described below. Because very weak peaks from the non-reflective quartz plate were observed in addition to those of $Mg_2Al_2O_5$ phase in the X-ray diffraction data, the quartz peaks were excluded in the Rietveld refinement.

3. Results and discussion

3.1. High-pressure phase transitions in $MgAl_2O_4$

Table 1 summarizes results of high pressure experiments in $MgAl_2O_4$ and $Mg_2Al_2O_5$ compositions, and the phase relations in $MgAl_2O_4$ are shown in Fig. 1. In $MgAl_2O_4$, the mixture of MgO periclase and Al_2O_3 corundum is stable up to about 26–27 GPa at temperatures of 1400–2000 °C. At higher pressure, calcium ferrite type $MgAl_2O_4$ becomes stable. The transition boundary between the two fields has a negative slope. The pressure and slope of the transition boundary are in general agreement with those in the previous study [1]. At pressure below 25.5 GPa above 2000 °C, we found a mixture of corundum and a new phase. Compositional analysis by SEM-EDS indicated that the new phase coexisting with corundum had Mg:Al ratio of 1:1 within analytical errors. To the best of our knowledge, a phase with $Mg_2Al_2O_5$ composition has not yet been reported. The powder X-ray diffraction profile of the mixture of corundum and the new $Mg_2Al_2O_5$ phase was different from that of ε-$MgAl_2O_4$ [5,6].

To examine the new $Mg_2Al_2O_5$ phase in more detail, we synthesized the new phase at 23.2 GPa and 2500 °C from the mixture of MgO and Al_2O_3 with 2:1 molar ratio (run no. N-6 in Table 1). The measured powder X-ray diffraction profile of the sample is shown in Fig. 2. After removing very weak quartz peaks, all of diffraction peaks in Fig. 2 were successfully indexed with orthorhombic symmetry and are shown in Table 2. As described in the next section, lattice parameters were determined by Rietveld refinement as $a = 9.3710(6)$ Å, $b = 12.1952(6)$ Å, $c = 2.7916(2)$ Å, and $V = 319.03(3)$ Å^3, and thus molar volume and density were calculated to be $V = 48.031(5)$ cm^3/mol and $\rho_{calc} = 3.801(1)$ g/cm^3, respectively, by adopting $Z = 4$. A part of the run product (N-6) was polished and analyzed by SEM-EDS. The result in Table 3 indicates that composition of the synthesized phase was $Mg_2Al_2O_5$ within the analytical errors. Using the powder X-ray diffraction profile of the new $Mg_2Al_2O_5$ phase, we concluded that the run products of $MgAl_2O_4$ synthesized at about 21–25.5 GPa and about 2000–2500 °C were the mixture of the $Mg_2Al_2O_5$ phase and corundum. The boundary between the field of MgO periclase and Al_2O_3 corundum and that of the $Mg_2Al_2O_5$ phase and corundum has a steep negative slope.

In Table 4, molar volumes and densities of $Mg_2Al_2O_5$ phase, $MgAl_2O_4$ polymorphs and related phase assemblages are compared. The molar volume of $Mg_2Al_2O_5$ phase is smaller only by

Table 1
Results of high-pressure experiments.

Run no.	Pressure (GPa)	Temperature (°C)	Time (min)	Phases[a]
$MgAl_2O_4$ composition				
S-4	27	1400	25	Per+Cor
S-3	27	1600	60	Cf+Cor+Per
S-27	26	1700	10	Per+Cor
S-5	26.5	1800	60	Cf+Cor+Per
S-2	27	1800	60	Cf
S-26	25.5	1900	10	Cf
S-34	21	2000	13	Per+Cor
S-19	23	2000	30	Per+Cor
W-2[b]	23	2000	3	Per+Cor
S-20	25	2000	30	Cor+Per +$Mg_2Al_2O_5$ Np
S-25	25.5	2000	5	Cor+$Mg_2Al_2O_5$ Np
S-24	26	2000	5	Cf
S-17	21	2100	10	Cor+$Mg_2Al_2O_5$ Np
S-16	23	2100	10	Cor+$Mg_2Al_2O_5$ Np
W-1[b]	23	2100	1	Cor+$Mg_2Al_2O_5$ Np
S-18	25	2100	10	Cor+$Mg_2Al_2O_5$ Np
S-21	25.5	2100	10	Cor+$Mg_2Al_2O_5$ Np
S-22	26	2100	10	$MgAl_2O_4$ Np
S-1	27	2100	60	Cf
S-12	25	2300	5	Cor+$Mg_2Al_2O_5$ Np
S-10	25.5	2300	5	Cor+$Mg_2Al_2O_5$ Np
S-13	26	2300	10	$MgAl_2O_4$ Np
S-14	26.5	2300	5	$MgAl_2O_4$ Np
S-7	27.2	2300	10	$MgAl_2O_4$ Np
S-10	23	2500	10	Cor+$Mg_2Al_2O_5$ Np
S-11	25	2500	5	Cor+$Mg_2Al_2O_5$ Np
S-9	25.5	2500	5	$MgAl_2O_4$ Np+Cor+$Mg_2Al_2O_5$ Np
S-8	26.5	2500	10	$MgAl_2O_4$ Np
S-6	27.2	2500	12	$MgAl_2O_4$ Np
$Mg_2Al_2O_5$ composition				
N-5	23.2	2500	1	$Mg_2Al_2O_5$ Np
N-6	23.2	2500	10	$Mg_2Al_2O_5$ Np
N-7	24	2500	4	$Mg_2Al_2O_5$ Np
N-8	24	2200	2	$Mg_2Al_2O_5$ Np
N-10	23	2500	1	$Mg_2Al_2O_5$ Np
N-11	23	2500	1	$Mg_2Al_2O_5$ Np

[a] Phases in the central part of each run product are shown. Per: periclase; Cor: corundum; Cf: calcium ferrite; and Np: new phase.
[b] Run nos. W-1 and W-2 were performed using the W-3%Re/W-25%Re thermocouple. In the other runs, the Pt/Pt-13%Rh thermocouple was used.

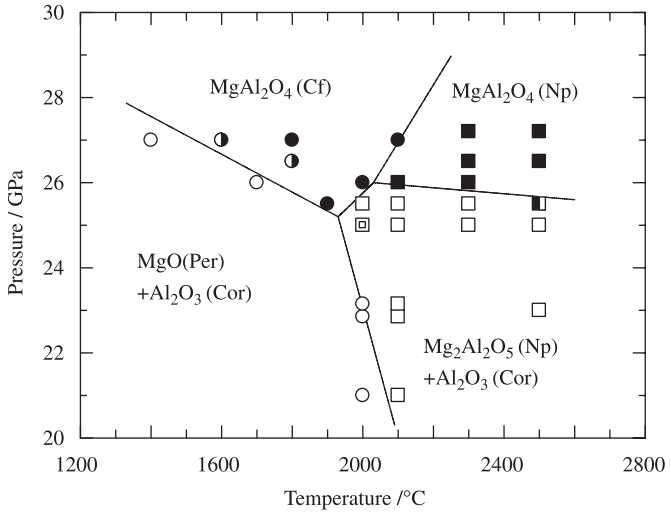

Fig. 1. Phase relations in $MgAl_2O_4$ at high pressures and high temperatures. Closed and open circles represent $MgAl_2O_4$ calcium ferrite and the assemblage of MgO periclase and Al_2O_3 corundum, respectively. Open squares indicate the mixture of the new $Mg_2Al_2O_5$ phase and Al_2O_3 corundum. An open double-square shows the mixture of the new $Mg_2Al_2O_5$ phase, Al_2O_3 corundum and MgO periclase. Closed squares indicate the new $MgAl_2O_4$ phase. Per: periclase, Cor: corundum, Cf: calcium ferrite, Np: new phase.

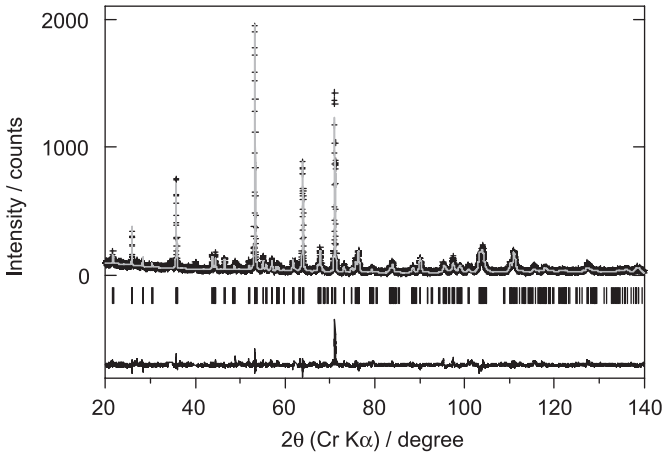

Fig. 2. Results of Rietveld refinement of $Mg_2Al_2O_5$ phase. Crosses and gray solid lines are the observed and calculated X-ray diffraction profiles, respectively. Vertical bars under the diffraction peaks show peak positions. The plots under the bars represent the differences between the observed and calculated patterns.

Table 2
Observed and calculated d values and relative intensities of the new $Mg_2Al_2O_5$ phase.

h	k	l	d_{obs}	d_{calc}	Relative intensity
0	2	0	6.1008	6.0976	4
1	2	0	5.1145	5.1109	13
1	3	0	3.7306	3.7293	34
2	3	0	3.0709	3.0705	6
3	1	0	3.0269	3.0260	6
1	4	0	2.9004	2.8992	5
0	0	1	2.7922	2.7916	1
3	2	0	2.7805	2.7801	2
1	1	1	2.6147	2.6133	3
2	4	0	2.5556	2.5554	100
3	3	0	2.4770	2.4769	5
1	2	1	2.4506	2.4500	2
2	0	1	2.3992	2.3982	4
1	5	0	2.3597	2.3604	3
4	0	0	2.3431	2.3428	2
2	2	1	2.2325	2.2318	4
2	5	0	2.1633	2.1635	46
2	3	1	2.0652	2.0655	3
3	1	1	2.0520	2.0518	10
0	6	0	2.0323	2.0325	2
3	2	1	1.9698	1.9699	73
3	5	0	1.9222	1.9224	3
2	6	0	1.8644	1.8647	6
3	3	1	1.8528	1.8527	9
4	2	1	1.7215	1.7215	3
1	7	0	1.7126	1.7128	5
4	3	1	1.6416	1.6417	3
1	6	1	1.6183	1.6185	6
2	6	1	1.5504	1.5506	4
0	8	0	1.5241	1.5244	6
5	2	1	1.5074	1.5077	3
1	8	0	1.5043	1.5046	3
5	5	0	1.4859	1.4861	3
1	7	1	1.4599	1.4599	2
6	3	0	1.4581	1.4579	3
5	3	1	1.4528	1.4532	6
0	0	2	1.3957	1.3958	4
6	4	0	1.3897	1.3901	10
6	1	1	1.3541	1.3546	4
4	8	0	1.2775	1.2777	5
5	7	0	1.2755	1.2760	2

The d_{calc} values were calculated using lattice parameters of $a = 9.3710(6)$ Å, $b = 12.1952(6)$ Å and $c = 2.7916(2)$ Å.

Table 3
Compositions of the two new phases in the system MgO–Al_2O_3.

	Run no. N-6 23.2 GPa, 2500 °C	Run no. S-6 27.2 GPa, 2500 °C
MgO	43.9(6)	28.5(1)
Al_2O_3	56.2(6)	71.5(1)
Total	100.1	100.0
O	5	4
Mg	1.98(2)	1.00(1)
Al	2.01(1)	2.00(1)
Total	3.99(2)	3.00(1)

Number in parentheses is two standard deviations of the mean.

0.18% than the sum (48.119 cm^3/mol) of 2MgO periclase and Al_2O_3 corundum. This very small volume difference may contribute to the steep gradient of the transition boundary between the field of MgO periclase+Al_2O_3 corundum to that of $Mg_2Al_2O_5$ phase+corundum in Fig. 1, because the boundary represents formation of $Mg_2Al_2O_5$ phase from periclase+corundum.

Generally, there is a temperature gradient in the sample of high-pressure experiment. In cylindrical run products, temperature is highest in the central part and lowest in the ends. Therefore, we can see change of stable phases with temperature along the axis of the cylindrical sample. In microfocus X-ray diffraction experiments of the run product S-25 synthesized at 25.5 GPa and 2000 °C, we observed $Mg_2Al_2O_5$ phase+corundum in the central part of sample, periclase+corundum in the ends, and $MgAl_2O_4$ calcium ferrite in between. However, in the run product S-20 at 25 GPa and 2000 °C, $Mg_2Al_2O_5$ phase+corundum+periclase were observed in the central part, and no calcium ferrite phase was observed in the sample. These results suggest that a triple point may exist at about 25 GPa and 1950 °C among the three fields of $Mg_2Al_2O_5$ phase+corundum, periclase+corundum, and calcium ferrite phase.

In the phase transition experiments of $MgAl_2O_4$, we found another new phase at pressure above about 26 GPa at temperature above 2100 °C. The powder X-ray diffraction data of the new $MgAl_2O_4$ phase are shown in Table 5. Results of compositional analysis of the run product S-6 in Table 3 synthesized at 27.2 GPa and 2500 °C indicated that the new phase had the composition of $MgAl_2O_4$ within the errors. The X-ray diffraction data of the $MgAl_2O_4$ phase are different from $MgAl_2O_4$ high-pressure phases previously found such as $CaTi_2O_4$-type [2] and ε-$MgAl_2O_4$ [5,6]. In addition, we could not find in literature any $A^{2+}B_2^{3+}O_4$ compound with a similar X-ray diffraction pattern to that of the present $MgAl_2O_4$ phase. Structural study on the $MgAl_2O_4$ phase is in progress. Based on the phases in run products synthesized at 26–27 GPa and 2000–2100 °C, we propose that another triple point may be present at around 26 GPa and 2050 °C among the fields of the new $MgAl_2O_4$ phase, calcium ferrite phase, and the mixture of $Mg_2Al_2O_5$ phase+corundum.

3.2. Structure analysis and Rietveld refinement of the new $Mg_2Al_2O_5$ phase

The powder X-ray diffraction data in Table 2 indicated systematic absence of $k = 2n+1$ for $0\,k\,l$ and $h = 2n+1$ for $h\,0\,l$. These suggested that the possible space group was *Pba2*(No. 32) or *Pbam*(No. 55). Comparing the lattice parameters and powder X-ray diffraction profile of the $Mg_2Al_2O_5$ phase with literature, we first chose the structure of ludwigite (Mg, Fe^{2+})$_2$(Fe^{3+}, Al)(BO_3)O_2 [13] as a starting structure model. In the ludwigite structure, boron is coordinated two-dimensionally by three oxygens. Because the boron sites are too small for Mg and Al of the $Mg_2Al_2O_5$ phase, the position was shifted by 0.5 along the *c*-axis. This treatment changed environment of this cation site from three-oxygen coordinated triangle to six-oxygen coordinated trigonal prism. This modified ludwigite structure belongs to a space group *Pbam*(No. 55). This structure model gave a very similar X-ray diffraction pattern to that observed for the $Mg_2Al_2O_5$ phase. To confirm validity of the above structure model, a possible structure was searched using the Structure Model-Assembly program [14]. This program automatically generates a structural model by Monte Carlo simulation and calculation of X-ray diffraction pattern. The search procedures established in the previous work [15] have been used for the present structural analysis. As a result, it was confirmed that the modified ludwigite structure described above gave the lowest *R*-factor in the search.

The Rietveld refinement was performed on the basis of the structure model of the modified ludwigite structure. Isotropic atomic displacement factors of all oxygen sites were fixed at 1.0. Those of five cation sites M1–M5 shown in Table 6 were fixed at

Table 4
Molar volumes and calculated densities of $Mg_2Al_2O_5$ phase, $MgAl_2O_4$ polymorphs, constituent oxides and their mixtures of $MgAl_2O_4$ composition.

Phase	Molar volume (cm^3/mol)	Density (g/cm^3)	Reference
$Mg_2Al_2O_5$	48.031(5)	3.801(1)	This study
$MgAl_2O_4$ spinel	39.760(3)	3.578(1)	[23]
$MgAl_2O_4$ calcium ferrite	36.136(3)	3.937(1)	[19]
MgO	11.266(5)	3.577(2)	[24]
Al_2O_3	25.587(1)	3.985(1)	[18]
$MgO+Al_2O_3$	36.853(5)	3.860(1)	[18,24]
$1/2(Mg_2Al_2O_5+Al_2O_3)$	36.809(3)	3.865(1)	This study [18]

Table 5
Powder X-ray diffraction data of the new $MgAl_2O_4$ phase.

d (Å)	Relative intensity
4.8691	50
3.8699	9
3.8358	7
3.3442	47
3.0626	4
2.7265	7
2.6518	38
2.5207	48
2.2994	4
2.2392	4
2.2288	3
2.1514	100
1.8048	4
1.7931	7
1.6227	62
1.5936	40
1.5062	20

Table 6
Lattice parameters and atomic positions of $Mg_2Al_2O_5$ phase determined by Rietveld refinement.

Space group: *Pbam*
$a = 9.3710(6)$ Å, $b = 12.1952(6)$ Å, $c = 2.7916(2)$ Å, $V = 319.03(3)$ Å^3, $Z = 4$

$R_{WP} = 17.6\%$, $R_I = 10.6\%$, $R_F = 6.5\%$, $R_e = 12.9\%$

Site		g (Mg)	g (Al)	x	y	z	B (Å^2)
M1	2*b*	0	1.0	0	0	1/2	1.0
M2	2*c*	0.8	0.2	1/2	0	0	1.0
M3	4*h*	0.3	0.7	0.9783(7)	0.2839(4)	1/2	0.7
M4	4*g*	0.3	0.7	0.2293(6)	0.1176(5)	0	0.7
M5	4*h*	1.0	0	0.2560(7)	0.3715(6)	1/2	1.5
O1	4*g*	–	–	0.1199(9)	0.9741(7)	0	1.0
O2	4*h*	–	–	0.1009(9)	0.1419(8)	1/2	1.0
O3	4*g*	–	–	0.0916(9)	0.3488(8)	0	1.0
O4	4*h*	–	–	0.3754(10)	0.0702(7)	1/2	1.0
O5	4*g*	–	–	0.3464(10)	0.2551(6)	0	1.0

$R_{WP} = \sqrt{\sum_i w_i[y_i(o) - y_i(c)]^2 / \sum_i w_i[y_i(o)]^2}$, $R_I = \sum_k |I_k(o) - I_k(c)| / \sum_k I_k(o)$.
$R_F = \sum_k |[I_k(o)]^{1/2} - [I_k(c)]^{1/2}| / \sum_k [I_k(o)]^{1/2}$ $R_e = \sqrt{(N-P)/\sum_i w_i[y_i(o)]^2}$.
The $y_i(o)$ and $y_i(c)$ are observed and calculated intensities at profile point i, respectively. The w_i is a weight for each step i. $I_k(o)$ and $I_k(c)$ are observed and calculated integrated intensities, respectively. N and P show numbers of data and of refined parameters, respectively.
g: site occupancy fraction.

empirical values which were refined with fixing the other ones. Site occupancy fractions of Mg and Al, g(Mg) and g(Al), in the cation sites were determined as the following procedure. Because the M1 and M5 sites are the smallest and largest sites, respectively, it was assumed that Al and Mg occupied selectively in the M1 and M5 sites, respectively, with 1.0 occupancy. Since the M3 and M4 sites are comparative in size, it was assumed that g(Mg) and g(Al) in the M3 sites were the same as those in the M4 sites. When site occupancy fractions in M2 site were varied, the minimum R factors of the refinement were obtained at g(Mg) of 0.8 and g(Al) of 0.2. Thus, we adopted the values for M2 site. They gave the g(Mg) of 0.3 and g(Al) of 0.7 for the M3 and M4 sites. In the refinement, site occupancy fractions were fixed at those values described above.

The results of the Rietveld refinement are shown in Tables 6 and 7 and Fig. 2. The residue in Fig. 2 and R factors suggest that the structure model of modified ludwigite is reasonably acceptable. In Fig. 2, the difference between the observed and calculated intensities of 321 reflection at 2θ of about 71° is relatively large. This is probably because preferred orientation effects were not perfectly removed in the refinement due to multiple preferred orientations. The refined structure is illustrated in Fig. 3. In the projection on the (0 0 1) plane, we can see zig-zag shapes of (Mg, Al)O_6 octahedra connected by edge-sharing. The zig-zag shapes of octahedra are connected each other by corner-sharing. The octahedra are also connected by edge-sharing to make a long chain along the c-axis. This sequence of octahedra is shown in Fig. 4. A space surrounded by the long chains forms a tunnel along the c-axis. This structure containing tunnels is similar to $CaFe_2O_4$ calcium ferrite structure [15], $KAlSi_3O_8$ hollandite structure [16], and hexagonal $CaMg_2Al_6O_{12}$ structure [17]. In these structures, the tunnels are surrounded by double-chains consisting of edge-sharing MO_6 octahedra. In the $Mg_2Al_2O_5$ structure, there are four kinds of octahedral sites, M1–M4. The six-coordinated M5 site placed in the tunnel is not an octahedral site but a trigonal prism, as shown in Fig. 4.

Refined interatomic distances and bond angles are listed in Table 7. In the M1 site, the average M1–O distance of 1.871 Å is slightly smaller than 1.914 Å for AlO_6 octahedra in Al_2O_3 corundum [18], 1.919 and 1.903 Å in $MgAl_2O_4$ calcium ferrite [19], and 1.919 Å in $CaMg_2Al_6O_{12}$ hexagonal aluminous phase [17]. However, it is comparable to the average Al–O distance of 1.887 Å in $Mg_3Al_2Si_3O_{12}$ pyrope [20]. The shortest M1–O distance (1.820 Å) is similar to the shortest Al–O distance of 1.828 Å in $Ca_2Al_2O_5$ brownmillerite [21].

The M5 site is the largest with the average M–O distance of 2.155 Å. This value is slightly larger than the average Mg–O distance of 2.078 Å for the Mg site in $CaMg_2Al_6O_{12}$ hexagonal aluminous phase, which has the same coordination environment of trigonal prism as the M5 site in the $Mg_2Al_2O_5$ phase. The sum (2.12 Å) of ionic radii [22] of O^{2-} and six-coordinated Mg^{2+} is in good agreement with the average M5–O distance.

The average M–O distances in the M2, M3 and M4 sites are obtained to be 2.019, 1.966 and 1.974 Å, respectively. These values

Table 7
Interatomic distances and bond angles in $Mg_2Al_2O_5$ phase.

M1 site		M2 site		M3 site		M4 site		M5 site	
Interatomic distance (Å)									
M1–O1 × 4	1.820(5)	M2–O4 × 4	2.011(6)	M3–O3 × 2	1.924(7)	M4–O2 × 2	1.866(7)	M5–O3 × 2	2.097(7)
M1–O2 × 2	1.973(9)	M2–O3 × 2	2.034(10)	M3–O5 × 2	1.924(7)	M4–O5	2.004(10)	M5–O5 × 2	2.164(8)
Average	1.871	Average	2.019	M3–O4	2.024(10)	M4–O1	2.029(9)	M5–O1 × 2	2.205(7)
				M3–O2	2.078(10)	M4–O4 × 2	2.039(7)	Average	2.155
				Average	1.966	Average	1.974		
Bond angle (degree)									
O1–M1–O2	81.8(3)	O3–M2–O4	98.1(3)	O2–M3–O3	92.2(4)	O4–M4–O5	82.5(4)	O1–M5–O1	78.5(3)
O1–M1–O1	100.2(4)	O4–M2–O4	87.9(4)	O2–M3–O5	98.6(4)	O2–M4–O5	102.7(5)	O3–M5–O3	80.4(3)
				O3–M3–O3	93.0(4)	O1–M4–O4	95.4(4)	O5–M5–O5	80.4(3)
				O5–M3–O5	93.0(5)	O1–M4–O2	79.1(4)	O1–M5–O5	75.9(3)
				O4–M3–O5	84.9(4)	O4–M4–O4	86.4(4)	O1–M5–O3	92.3(3)
				O3–M3–O4	84.3(4)	O2–M4–O2	96.8(5)	O3–M5–O5	76.8(3)
				O2–M3–O4	174.9(6)	O1–M4–O5	177.1(5)		

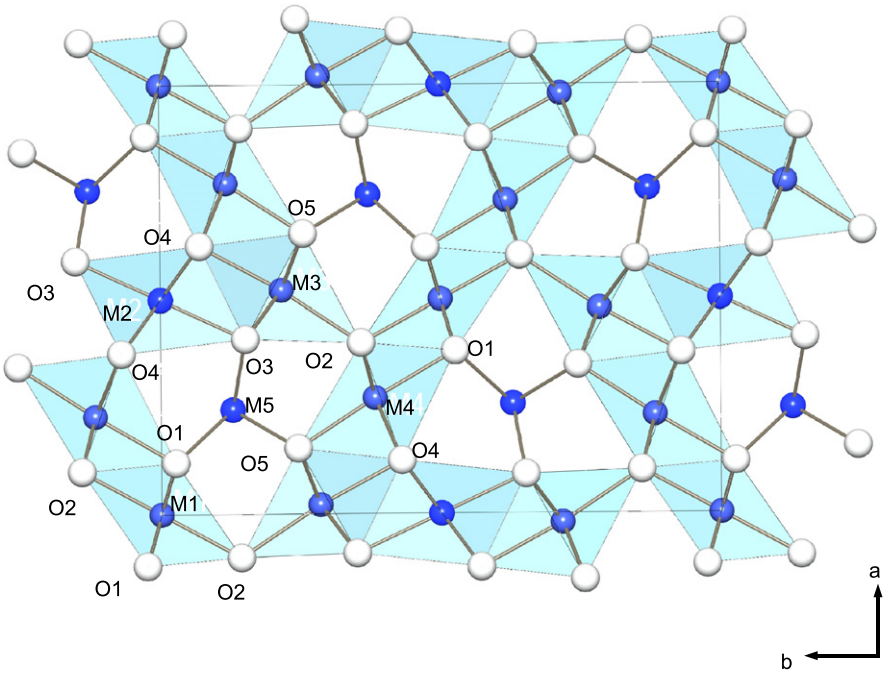

Fig. 3. Crystal structure of $Mg_2Al_2O_5$ phase projected on (0 0 1) plane. White and blue balls indicate oxygen and cation (Mg or Al) sites, respectively. (Mg, Al)O_6 octahedra are represented with light blue color. A rectangle shows unit cell dimension.

are intermediate between those of the M1 and M5 sites. This indicates that both of Mg^{2+} and Al^{3+} may occupy the M2, M3 and M4 sites with some ratios. In fact, structure models in which a site among the M2, M3 and M4 sites was occupied by only Mg^{2+} or Al^{3+} gave 2–3% larger R factors than the model used for the Rietveld refinement. The fact supported the model with distribution of both Mg^{2+} and Al^{3+} among the M2, M3 and M4 sites.

It is interesting that $Mg_2Al_2O_5$ has the modified ludwigite structure at high pressure, while $Ca_2Al_2O_5$ crystallizes in brownmillerite structure at 2.5 GPa [21]. The brownmillerite structure is regarded as an oxygen-defect perovskite structure. In the brownmillerite-type $Ca_2Al_2O_5$ [21], Ca is in eight-fold coordinated site and Al in ordered tetrahedral and octahedral sites. It is likely that $Mg_2Al_2O_5$ crystallizes into the modified ludwigite structure because, compared with Ca, Mg is too small to be accommodated in the brownmillerite structure.

Our study has shown that $MgAl_2O_4$ dissociates into a mixture of Al_2O_3 corundum and $Mg_2Al_2O_5$ with the new structure. This type of high-pressure dissociation has been found only in $MgAl_2O_4$ among various $A^{2+}B_2^{3+}O_4$ phases. A calorimetric study on this type of dissociation would be interesting for understanding of energetics of high-pressure phases in the system MgO–Al_2O_3. Also, further systematic study on high-pressure transitions in $A^{2+}B_2^{3+}O_4$ would increase a wealth of our knowledge on crystal chemistry of $A^{2+}B_2^{3+}O_4$ compounds.

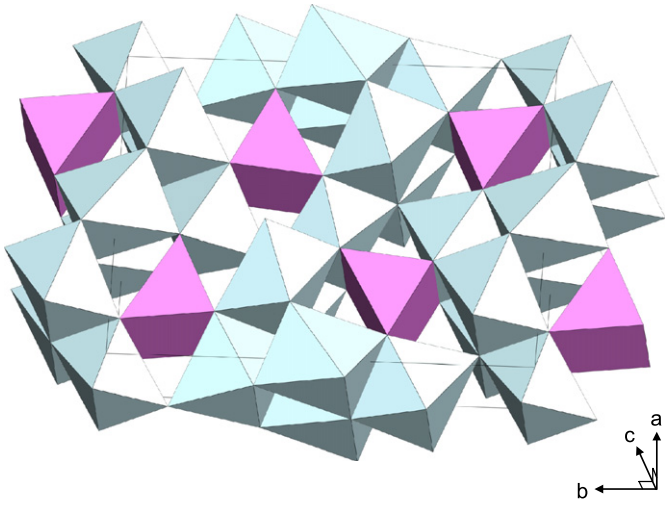

Fig. 4. Crystal structure of $Mg_2Al_2O_5$ phase illustrated with coordination polyhedra. MgO_6 trigonal prisms (purple) are placed in triangular tunnels surrounded by (Mg, Al)O_6 octahedra.

Acknowledgments

We are grateful to two anonymous reviewers for constructive comments. This work was partially supported by Grants-in-aid (no. 19340166 to M. A. and no. 18540478 to H. K.) from the Japan Society for the Promotion of Science.

References

[1] M. Akaogi, Y. Hamada, T. Suzuki, M. Kobayashi, M. Okada, Phys. Earth Planet. Inter. 115 (1999) 67–77.
[2] N. Funamori, R. Jeanloz, J.H. Nguyen, A. Kavner, W.A. Caldwell, K. Fujino, N. Miyajima, T. Shinmei, N. Tomioka, J. Geophys. Res. 103 (1998) 20813–20818.
[3] K. Yamaura, Q. Huang, M. Moldovan, D.P. Young, A. Sato, Y. Baba, T. Nagai, Y. Matsui, E. Takayama-Muromachi, Chem. Mater. 17 (2005) 359–365.
[4] K. Yamaura, M. Arai, A. Sato, A.B. Karki, D.P. Young, R. Movshovich, S. Okamoto, D. Mandrus, E. Takayama-Muromachi, Phys. Rev. Lett. 99 (2007) 196601–196604.
[5] L.G. Liu, Earth Planet. Sci. Lett. 41 (1978) 398–404.
[6] S. Ono, T. Kikegawa, Y. Ohishi, Phys. Chem. Minerals 32 (2006) 200–2006.
[7] H. Morishima, T. Kato, M. Suto, E. Ohtani, S. Urakawa, W. Utsumi, O. Shimomura, T. Kikegawa, Science 265 (1994) 1202–1203.
[8] A. Suzuki, E. Ohtani, H. Morishima, T. Kubo, Y. Kanbe, T. Kondo, T. Okada, H. Terasaki, T. Kato, T. Kikegawa, Geophys. Res. Lett. 27 (2000) 803–806.
[9] S. Ono, T. Katsura, E. Ito, M. Kanzaki, A. Yoneda, M.J. Walter, S. Urakawa, W. Utsumi, K. Funakoshi, Geophys. Res. Lett. 28 (2001) 835–838.
[10] K. Hirose, Y. Fei, S. Ono, T. Yagi, K. Funakoshi, Earth Planet. Sci. Lett. 184 (2001) 567–573.
[11] M. Akaogi, A. Tanaka, E. Ito, Phys. Earth Planet. Inter. 132 (2002) 303–324.
[12] F. Izumi, T. Ikeda, Mater. Sci. Forum 321–324 (2000) 198–204.
[13] Y. Takeuchi, T. Watanabe, T. Ito, Acta Cryst. 3 (1950) 98–107.
[14] H. Miura, T. Kikuchi, J. Chem. Software 5 (1999) 163–172.
[15] B.F. Decker, J.S. Kasper, Acta Cryst. 10 (1957) 332–337.
[16] H. Yamada, Y. Matsui, E. Ito, Mineral. J. 12 (1984) 29–34.
[17] H. Miura, Y. Hamada, T. Suzuki, M. Akaogi, N. Miyajima, K. Fujino, Am. Mineral. 85 (2000) 1799–1803.
[18] D.M. Toebbens, N. Stuesser, K. Knorr, H.M. Myer, G. Lampert, Mater. Sci. Forum 378 (2001) 288–293.
[19] H. Kojitani, R. Hisatomi, M. Akaogi, Am. Mineral. 92 (2007) 1112–1118.
[20] R.M. Hazen, L.W. Finger, Am. Mineral. 63 (1978) 297–303.
[21] V. Kahlenberg, R.X. Fischer, C.S.J. Shaw, Am. Mineral. 85 (2000) 1061–1065.
[22] R.D. Shannon, C.T. Prewitt, Acta Cryst. B 25 (1969) 925–946.
[23] F. Meducin, S.A.T. Redfern, Y. Le Godec, H.J. Stone, M.G. Tucker, M.T. Dove, W.G. Marshall, Am. Mineral. 89 (2004) 981–986.
[24] V.G. Tsirelson, A.S. Avilov, Y.A. Abramov, E.L. Belokoneva, R. Kitaneh, D. Feil, Acta Cryst. B 54 (1998) 8–17.